

methods would give very similar results if the basis set were exhausted, but this is not done in the latter calculation here. The additional relaxation due to the inclusion of the higher energy virtual orbitals in the extended 2ph-TDA calculation would move the ionization energies down and put them into closer agreement with the OVG results. The nearly perfect agreement with experiment thus results from the limited number of virtual orbitals that were taken into account.

Electron ejection from the  $1t_2$  and  $1a_1$  orbitals, which are essentially combinations of the Cl 3s atomic orbitals, cannot be described within a one-particle picture. Here a strong mixing of ionization with ionization plus excitation processes occurs, leading to the strong splitting of the lines. The extended 2ph-TDA results are given in Table I and are graphically represented in Figure 1, which contains as an insert also the He I photoelectron spectrum from ref 6. For  $1t_2$  ionization the maximum pole strength of a component is obtained as 0.2, and for  $1a_1$  ionization it is obtained as 0.26. The 2h1p configurations, which couple strongly with the simple hole configurations, involve as particle states the 2e,  $3a_1$ , and most important, the  $4t_2$ ,  $5t_2$ , and  $6t_2$  orbitals. The 2e orbital is built up from Cl p and Ti d functions, and the other ones are built from Cl s and p and Ti p and d functions. In many cases the Ti d participation is strong. To a certain degree this can be interpreted as a repopulation of the d orbitals on Ti, but this should not be overemphasized as the splitting of the Cl 3s lines is a general phenomenon (see references in ref 24) and is independent of the presence or absence of a transition-metal atom. The results obtained in this energy range are only qualitative or semiquantitative for several reasons. One of them has been mentioned above. In this case the ionic states are dominated by 2h1p configurations and the extended 2ph-TDA method gives only results that are accurate to first order of perturbation theory.<sup>22</sup> To improve this, one has to include the 3h2p and 3p2h configurations (i.e. the double excitations on top of the simple hole and simple particle states) in addition to the 2h1p and 2p1h configurations, which are included in the present calculation. Such a theory has been developed,<sup>22</sup> and a simplified version is being applied to some small molecules.<sup>33</sup> However, the  $\text{TiCl}_4$  molecule is just slightly too large for the application of this high-order and demanding theory. A second reason is the following one. In the inner-valence region, where we find this splitting of lines, we also find the

double-ionization threshold, which for  $\text{TiCl}_4$  probably lies between 30 and 40 eV. An infinite number of Rydberg states of the ion converge to this threshold. To describe them properly would require an extremely large basis set. Since this cannot be done, one does not calculate true eigenstates but pseudostates, which give only a rough idea of the spectral distribution. It has also been found for the  $\text{Cl}_2$  and the HCl molecules<sup>34,35</sup> that d-type functions are necessary to describe this part of the spectrum. Experimental information on this energy range is scarce or unavailable for  $\text{TiCl}_4$ , but more and more information is being obtained by (e,2e) spectroscopy<sup>36,37</sup> and synchrotron radiation,<sup>38,39</sup> which together with theoretical calculations help to develop an understanding of the process in this interesting energy range.

### Summary

The ionization energies of  $\text{TiCl}_4$  are calculated in the outer- and inner-valence regions by ab initio many-body Green's function methods, which include the effect of electron correlation and relaxation. The first five ionization processes can be well-described in the molecular orbital model of ionization. The calculated ionization energies lead to the assignment of the photoelectron spectral bands A, B, (C + D), and E as  $1t_1$ ,  $3t_2$ , ( $1e + 2t_2$ ), and  $2a_1$ . For  $1t_2$  and  $1a_1$  ionization we observe the breakdown of the molecular orbital model of ionization and the intensity becomes distributed over many lines, which carry only a small fraction of the intensity associated with these ionizations.

**Acknowledgment.** The calculations were performed on the Amdahl 470/V7b computer of the Computing Center of the Technical University of Braunschweig, whose service I gratefully acknowledge. I thank the Fonds der Chemischen Industrie for partial support of this work.

(33) von Niessen, W.; Tomasello, P.; Schirmer, J.; Cederbaum, L. S. *Aust. J. Phys.*, in press.

- (34) Brion, C. E.; Frost, L.; Grisogono, A. M.; Weigold, E.; McCarthy, I. E.; Bawagan, A. O.; Mukherjee, P. K.; von Niessen, W.; Sgamellotti, A., manuscript in preparation.  
 (35) von Niessen, W., unpublished results.  
 (36) McCarthy, I. E.; Weigold, E. *Phys. Rep.* **1976**, *27C*, 275.  
 (37) Weigold, E.; McCarthy, I. E. *Adv. At. Mol. Phys.* **1978**, *14*, 127.  
 (38) Kunz, C., Ed. *Synchrotron Radiation*; Springer-Verlag: Heidelberg, 1979.  
 (39) Koch, E. E., Ed. *Handbook of Synchrotron Radiation*; North-Holland: Amsterdam, 1983; Vol. 1.  
 (40) Lübcke, M.; Sonntag, B.; Wetzel, H. E. *Conference Proceedings, International Conference on X-ray and Inner-Shell Processes in Atoms, Molecules, and Solids*; Meisel, A., Ed.; Karl-Marx-Universität: Leipzig, 1984; Abstracts Part I, p 281. Lübcke, M. Ph.D. Thesis, Hamburg, 1984. Wetzel, H. E. Ph.D. Thesis, Hamburg, in preparation.

Contribution from the Department of Chemistry,  
York University, North York, Ontario, Canada M3J 1P3

## Electrochemistry and Spectroelectrochemistry of Mononuclear and Binuclear Cobalt Phthalocyanines

W. A. Nevin, M. R. Hempstead, W. Liu,<sup>1</sup> C. C. Leznoff, and A. B. P. Lever\*

Received August 8, 1986

The electrochemistry of (2,9,16,23-tetraneopentoxophthalocyanato)cobalt, and some binuclear analogues, has been studied in dichlorobenzene and in dimethylformamide. The redox mechanisms and species on the electrode are discussed. With the use of an optically thin electrode, the electronic spectra of seven different oxidation states of the mononuclear derivative are reported. Data for a selection of oxidation states of several binuclear species are also presented.

### Introduction

The electrochemistry and spectroelectrochemistry of metalloporphyrins have been extensively studied.<sup>2-16</sup> However, relatively

little spectroelectrochemistry has been carried out on phthalocyanines<sup>17-25</sup> due to their low solubilities in suitable solvents for

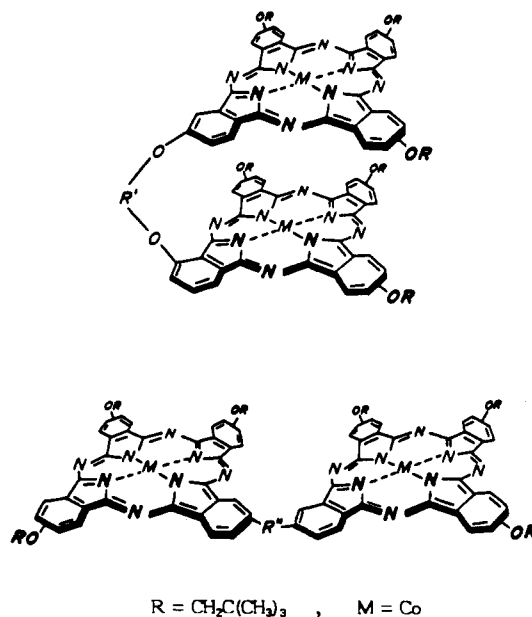
- (1) Current address: Department of Chemistry, Yangzhou Teachers' College, Yangzhou, Jiangsu, People's Republic of China.  
 (2) Fajer, J.; Borg, D. C.; Forman, A.; Dolphin, D.; Felton, R. H. *J. Am. Chem. Soc.* **1970**, *92*, 3451.  
 (3) Wolberg, A.; Manassen, J. *J. Am. Chem. Soc.* **1970**, *92*, 2982.

- (4) Truxillo, L. A.; Davis, D. G. *Anal. Chem.* **1975**, *47*, 2260.  
 (5) Lin, X. Q.; Kadish, K. M. *Anal. Chem.* **1985**, *57*, 1498.  
 (6) Kelly, S.; Lancon, D.; Kadish, K. M. *Inorg. Chem.* **1984**, *23*, 1451.  
 (7) Walker, F. A.; Beroiz, D.; Kadish, K. M. *J. Am. Chem. Soc.* **1976**, *98*, 3484.  
 (8) Felton, R. H.; Linschitz, L. *J. Am. Chem. Soc.* **1966**, *88*, 1113.  
 (9) Psychal-Heiling, G.; Wilson, G. S. *Anal. Chem.* **1971**, *43*, 550.

electrochemistry, which limits the use of optically transparent thin-layer electrodes (OTTE). Such studies are desirable in view of the potential use of phthalocyanines as electrocatalysts,<sup>26-28</sup> where an understanding of the nature of the redox processes of the phthalocyanine molecule is essential for the design of more efficient catalysts. The redox processes may occur at either the central metal atom or the phthalocyanine ring, but this cannot usually be distinguished by using electrochemistry alone. Spectroelectrochemical studies of the phthalocyanines are also important with regard to their possible use as electrochromic materials.<sup>24,29,30</sup>

Recently,<sup>31-33</sup> we have reported the synthesis of a series of binuclear phthalocyanines formed by linking units of trineopentoxypthalocyanine (TrNPc) together through a benzene ring by bridges of one, two, four, or five atoms. The three neopentoxy groups are randomly distributed in the 4- or 5-positions of the unlinked benzene rings and provide high solubility for the phthalocyanines in a wide range of organic solvents, such as toluene, *o*-dichlorobenzene (DCB), dichloromethane (DCM), and *N,N*-dimethylformamide (DMF). These complexes, in particular the cobalt derivatives, have been the subject of recent investigations as oxygen reduction catalysts and as multielectron redox catalysts.<sup>26,34</sup> We report here an electrochemical and spectroelectrochemical study on the cobalt derivatives of mononuclear and binuclear neopentoxypthalocyanines in DCB and DMF.

The purpose of this work was to obtain, for the first time, the electronic spectra of a wide range of electrochemically generated CoPc redox species in organic solution and, in addition, to determine any possible effects of coupling in the binuclear species on the redox processes and spectra. Several scattered reports of CoPc redox species exist in the literature; however, these are



- A
- EtMeO(5)[CoTrNPc]<sub>2</sub>, R' = CH<sub>2</sub>C(CH<sub>3</sub>CH<sub>2</sub>)(CH<sub>2</sub>)CH<sub>2</sub>
- Cat(4)[CoTrNPc]<sub>2</sub>, R' = *o*-phenylene
- B
- C(2)[CoTrNPc]<sub>2</sub>, R'' = CH<sub>2</sub>CH<sub>2</sub>
- O(1)[CoTrNPc]<sub>2</sub>, R'' = O

Figure 1. Binuclear phthalocyanine compounds.

incomplete and are often reported in the solid state where Davydov effects will disturb the spectra.

Spectra are presented here for a series of seven electrochemically generated redox species of the mononuclear derivative.

Of relevance to this presentation are the following species, with their abbreviations (Figure 1) (the number in parentheses is the number of bridging atoms connecting the two phthalocyanine rings): CoTNPc, (2,9,16,23-tetraneopentoxypthalocyanato)cobalt (the mononuclear control molecule); EtMeO(5)[CoTrNPc]<sub>2</sub>, phthalocyanine rings linked via -OCH<sub>2</sub>C(Me)(Et)CH<sub>2</sub>O-; Cat(4)[CoTrNPc]<sub>2</sub>, phthalocyanine rings linked via -OC<sub>6</sub>H<sub>4</sub>O- (*o*-catechol); C(2)[CoTrNPc]<sub>2</sub>, phthalocyanine rings linked via -CH<sub>2</sub>CH<sub>2</sub>-; O(1)[CoTrNPc]<sub>2</sub>, phthalocyanine rings linked via a single oxygen (ether) bridge.

These binuclear complexes can exist in various conformations depending upon the nature of the bridging unit.<sup>35</sup> The EtMeO(5) and Cat(4) species can close in a "clamshell"-like fashion (see Figure 1), while geometrical constraints of the bridge restrict the C(2) and O(1) species to an open conformation. Electronic coupling between the phthalocyanine rings may occur through space or through the bridge.<sup>35</sup> For the series of binuclear cobalt derivatives, the degree of electronic interaction between the phthalocyanine rings has been found to increase in the order<sup>34</sup> C(2) < EtMeO(5) < Cat(4) < O(1).

The nomenclature CoTNPc or [CoTrNPc]<sub>2</sub> is used for a general species of undefined oxidation state, while for specific compounds, the oxidation states of both metal and phthalocyanine are defined. The Pc(-2) state is the standard oxidation state for the phthalocyanine ring.<sup>36,37</sup>

- (10) Fuhrhop, J.-H.; Kadish, K. M.; Davis, D. G. *J. Am. Chem. Soc.* **1973**, *95*, 5140.
- (11) Brown, G. M.; Hopf, F. R.; Ferguson, J. A.; Meyer, T. J.; Whitten, D. G. *J. Am. Chem. Soc.* **1973**, *95*, 5939.
- (12) Kelly, S. L.; Kadish, K. M. *Inorg. Chem.* **1984**, *23*, 679.
- (13) Collman, J. P.; Marrocco, M.; Elliot, C. M.; L'Her, M. *J. Electroanal. Chem. Interfacial Electrochem.* **1981**, *124*, 113.
- (14) Le Mest, Y.; L'Her, M.; Courtot-Coupez, J.; Collman, J. P.; Evitt, E. R.; Bencosme, C. S. *J. Electroanal. Chem. Interfacial Electrochem.* **1985**, *184*, 331.
- (15) Felton, R. H. In *The Porphyrins*; Dolphin, D., Ed.; Academic: New York, 1978; Vol. V, Chapter 3.
- (16) Davis, D. G. In *The Porphyrins*; Dolphin, D., Ed.; Academic: Press: New York, 1978; Vol. V, Chapter 4.
- (17) Nevin, W. A.; Liu, W.; Melnik, M.; Lever, A. B. P. *J. Electroanal. Chem. Interfacial Electrochem.* **1986**, *213*, 217.
- (18) Lever, A. B. P.; Wilshire, J. P. *Inorg. Chem.* **1978**, *17*, 1145.
- (19) Rollmann, L. D.; Iwamoto, R. T. *J. Am. Chem. Soc.* **1968**, *90*, 1455.
- (20) Clack, D. W.; Yandle, J. R. *Inorg. Chem.* **1972**, *11*, 1738.
- (21) Dolphin, D.; James, B. R.; Murray, A. J.; Thornback, J. R. *Can. J. Chem.* **1980**, *58*, 1125.
- (22) Ferraudi, G.; Oishi, S.; Muralidharan, S. *J. Phys. Chem.* **1984**, *88*, 5261.
- (23) Bottomley, L. A.; Gorce, J.-N.; Goedken, V. L.; Ercolani, C. *Inorg. Chem.* **1985**, *24*, 3733.
- (24) Gavrilov, V. I.; Tomilova, L. G.; Shelepin, I. V.; Luk'yanets, E. A. *Elektrokhimiya* **1979**, *15*, 1058.
- (25) Kobayashi, N.; Shirai, H.; Hojo, N. *J. Chem. Soc., Dalton Trans.* **1984**, 2107. Kobayashi, N.; Nishiyama, Y. *J. Phys. Chem.* **1985**, *89*, 1167.
- (26) Hempstead, M. R.; Lever, A. B. P.; Leznoff, C. C., to be submitted for publication.
- (27) Lieber, C. M.; Lewis, N. S. *J. Am. Chem. Soc.* **1984**, *106*, 5033.
- (28) Hirai, T.; Yamaki, J. *J. Electrochem. Soc.* **1985**, *132*, 2125. Simic-Glavaski, B.; Zecevic, S.; Yeager, E. *J. Electroanal. Chem. Interfacial Electrochem.* **1983**, *150*, 469; *J. Phys. Chem.* **1983**, *87*, 4555.
- (29) Collins, G. C. S.; Schiffrin, D. J. *J. Electroanal. Chem. Interfacial Electrochem.* **1982**, *139*, 335. M'Sadak, M.; Roncali, J.; Garnier, F. *J. Electroanal. Chem. Interfacial Electrochem.* **1985**, *189*, 99.
- (30) Nicholson, M. M.; Pizzarello, F. A. *J. Electrochem. Soc.* **1981**, *128*, 1288, 1740.
- (31) Leznoff, C. C.; Greenberg, S.; Marcuccio, S. M.; Minor, P. C.; Seymour, P.; Lever, A. B. P.; Tomer, K. B. *Inorg. Chim. Acta* **1984**, *89*, L35. Leznoff, C. C.; Marcuccio, S. M.; Greenberg, S.; Lever, A. B. P.; Tomer, K. B. *Can. J. Chem.* **1985**, *63*, 623.
- (32) Marcuccio, S. M.; Svirskaya, P. I.; Greenberg, S.; Lever, A. B. P.; Leznoff, C. C.; Tomer, K. B. *Can. J. Chem.* **1985**, *63*, 3057.
- (33) Greenberg, S.; Marcuccio, S. M.; Leznoff, C. C.; Tomer, K. B. *Synthesis* **1986**, 406.
- (34) Liu, W.; Nevin, W. A.; Hempstead, M. R.; Melnik, M.; Lever, A. B. P.; Leznoff, C. C., submitted for publication in *J. Chem. Soc., Dalton Trans.*

(35) Dodsworth, E. S.; Lever, A. B. P.; Seymour, P.; Leznoff, C. C. *J. Phys. Chem.* **1985**, *89*, 5698.

(36) The symbol Pc(-2) refers to the dinegatively charged phthalocyanine unit in its standard oxidation state. The first ring-oxidized species is the radical Pc(-1), and the first ring-reduced species is the radical Pc(-3).<sup>37</sup>

**Table I.** Electrochemical Data for Mononuclear and Binuclear Neopentoxypthalocyanines

compd	$E_{1/2}$ , V ( $\Delta E_p$ , mV) <sup>a</sup>				
	oxidn			redn	
	I	II <sup>c</sup>	III	IV	V
H <sub>2</sub> TNPc	+0.77		+0.28	-1.35	-1.70 (70)
CoTNPc	+0.87 (102)	+0.59 (90)	+0.03 (89)	-0.91 (70)	-2.07 (80)
CoTNPc <sup>b</sup>		+0.38 <sup>d</sup>	-0.02	-0.85 (85)	-1.99 (85)
EtMeO(5)[CoTrNPc] <sub>2</sub>	+0.87	<i>e</i>	+0.05 (165)	-0.93	-2.07 (85)
Cat(4)[CoTrNPc] <sub>2</sub>	+0.89	<i>e</i>	+0.03	-0.93	-2.07 (95)
C(2)[CoTrNPc] <sub>2</sub> <sup>f</sup>	+0.87	+0.33	+0.03	-0.94	-2.07
O(1)[CoTrNPc] <sub>2</sub> <sup>f</sup>	+0.91	+0.51	+0.04	-0.93	-2.07

<sup>a</sup>DCB solution except as otherwise noted. Potentials are reported with respect to the ferrocenium/ferrocene couple.  $E_{1/2}$  values measured by cyclic voltammetry at 100, 50, and 20 mV/s [ $E_{1/2} = (E_{pa} + E_{pc})/2$ ] or differential-pulse polarography at 2 mV/s gave essentially identical potentials. Values of  $\Delta E_p$  ( $=E_{pa} - E_{pc}$ ) are given for a potential sweep rate of 20 mV/s. See text for assignment of couples I-V. <sup>b</sup>DMF solution. <sup>c</sup>The potential of this couple in DCB is very sensitive to traces of coordinating anions. <sup>d</sup>Weak shoulder at 0.30 V, see text, assigned to couple II'. <sup>e</sup>Not resolved. <sup>f</sup>Additional weak waves are seen at -1.36 and -1.7 V as a consequence of aggregation.

### Experimental Section

The species H<sub>2</sub>TNPc,<sup>31</sup> CoTNPc,<sup>31</sup> EtMeO(5)[CoTrNPc]<sub>2</sub>,<sup>31</sup> Cat(4)[CoTrNPc]<sub>2</sub>,<sup>32</sup> C(2)[CoTrNPc]<sub>2</sub>,<sup>32</sup> and O(1)[CoTrNPc]<sub>2</sub><sup>33</sup> were prepared by the literature routes cited. *N,N*-Dimethylformamide (DMF) (Aldrich, Gold Label, anhydrous, H<sub>2</sub>O < 0.005%, packaged under nitrogen), *o*-dichlorobenzene (DCB) (Aldrich, Gold Label), dichloromethane (DCM) (Aldrich, Gold Label), and acetonitrile (Aldrich, Gold Label) were used as supplied. Tetrabutylammonium perchlorate (TBAP) (Kodak) was recrystallized from absolute ethanol and dried at 50 °C under vacuum for 2 days. [Co<sup>III</sup>(CN)<sub>2</sub>TNPc(-2)]K<sup>38-40</sup> was prepared by adding a 10-fold excess of KCN to a solution of Co<sup>II</sup>TNPc(-2) in DCM/CH<sub>3</sub>CN (2:1).

Electronic spectra were recorded with a Hitachi Perkin-Elmer Microprocessor Model 340 spectrometer or a Guided Wave Inc. Model 100-20 optical waveguide spectrum analyzer with a WW100 fiber optic probe. Electrochemical data were obtained with a Pine Model RDE 3 double potentiostat, or a Princeton Applied Research (PARC) Model 173 potentiostat, or a PARC Model 174A polarographic analyzer coupled to a PARC Model 175 universal programmer. Cyclic voltammetry and differential-pulse polarography were carried out under an atmosphere of nitrogen in a Vacuum Atmospheres Drilab by using a conventional three-electrode cell. A platinum disk described by the cross-sectional area of a 27-gauge wire (area ca. 10<sup>-3</sup> cm<sup>2</sup>), sealed in glass, was used as the working electrode in DCB solution, and a platinum wire was used in DMF solution. A platinum wire served as the counter electrode, and a silver wire was used as a quasi-reference electrode. Potentials were referenced internally to the ferrocenium/ferrocene (Fc<sup>+</sup>/Fc) couple (+0.16 V vs. SCE).<sup>41</sup> All DMF solutions were prepared within the drybox. The DCB solutions were prepared in air, degassed by repeated freeze-pump-thaw cycles, and then transferred to the drybox.

Spectroelectrochemical measurements were made with an optically transparent thin-layer electrode cell, utilizing a gold minigrad (500 lines/in.),<sup>42</sup> in conjunction with the Hitachi Perkin-Elmer spectrometer or by using a bulk electrolysis cell, consisting of a platinum-plate working electrode, platinum-flag counter electrode, and silver-wire quasi-reference electrode (reference and counter electrodes were separated from the working compartment by medium glass frits). Spectra were recorded during bulk electrolysis by immersing the Guided Wave fiber optic probe in the solution, degassed with argon.

Solutions for electrochemistry and spectroelectrochemistry contained 0.1–0.3 M TBAP, as supporting electrolyte.

### Results and Discussion

**Electrochemistry in DCB Solution.** Figure 2a shows a typical cyclic voltammogram of CoTNPc in DCB. The molecule undergoes two quasi-reversible one-electron reductions and three quasi-reversible one-electron oxidations within the limit of the solvent ( $i_a = i_c$ ,  $i \propto v^{1/2}$ ). Half-wave potentials and peak separations at a scan rate ( $v$ ) of 20 mV/s are given in Table I.

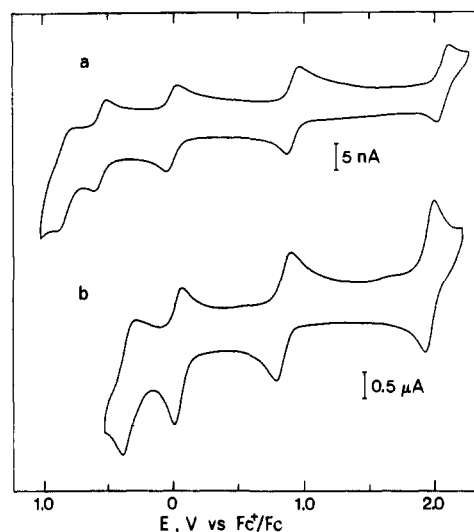


**Figure 2.** Cyclic voltammetry of CoTNPc (a) in DCB solution (Pt-disk working electrode) and (b) in DMF solution (Pt-wire working electrode). Scan rate = 50 mV/s, [CoTNPc] = 1 × 10<sup>-4</sup> M, and [TBAP] = 0.3 M.

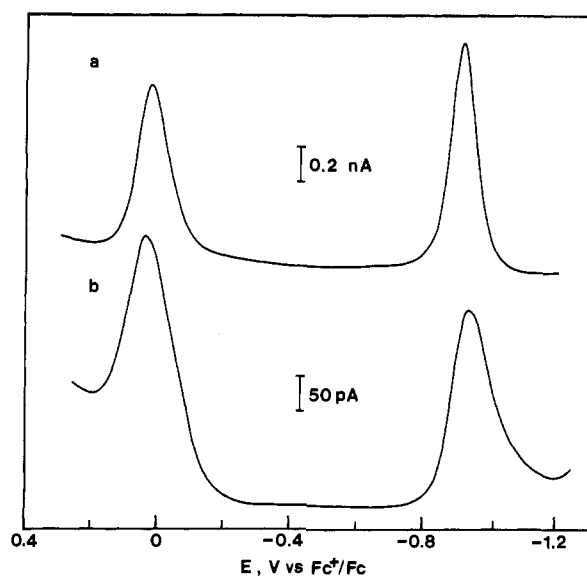


**Figure 3.** Differential-pulse polarograms of (a) CoTNPc and (b) O(1)[CoTrNPc]<sub>2</sub> in DCB solution (0.3 M TBAP). Scan rate = 2 mV/s, [CoTNPc] = 1 × 10<sup>-4</sup> M, and [O(1)[CoTrNPc]<sub>2</sub>] = ca. 5 × 10<sup>-5</sup> M.

The binuclear [CoTrNPc]<sub>2</sub> complexes show voltammetry very similar to that of the mononuclear species, although the waves are generally broader and weaker. However, well-defined peaks were obtained by differential-pulse polarography; Figure 3 compares the results for O(1)[CoTrNPc]<sub>2</sub> with those of CoTNPc in

(37) Myers, J. F.; Rayner-Canham, G. W.; Lever, A. B. P. *Inorg. Chem.* **1975**, *14*, 461.

(38) Metz, J.; Hanack, M. *J. Am. Chem. Soc.* **1983**, *105*, 828.

(39) Day, P.; Hill, H. A. O.; Price, M. G. *J. Chem. Soc. A* **1968**, 90.

(40) Stillman, M. J.; Thompson, A. J. *J. Chem. Soc., Faraday Trans. 2* **1974**, *70*, 790.

(41) Gagne, R. R.; Koval, C. A.; Lisensky, G. C. *Inorg. Chem.* **1980**, *19*, 2854. Gritzner, G.; Kuta, J. *Electrochim. Acta* **1984**, *29*, 869.

(42) Nevin, W. A.; Lever, A. B. P., to be submitted for publication.

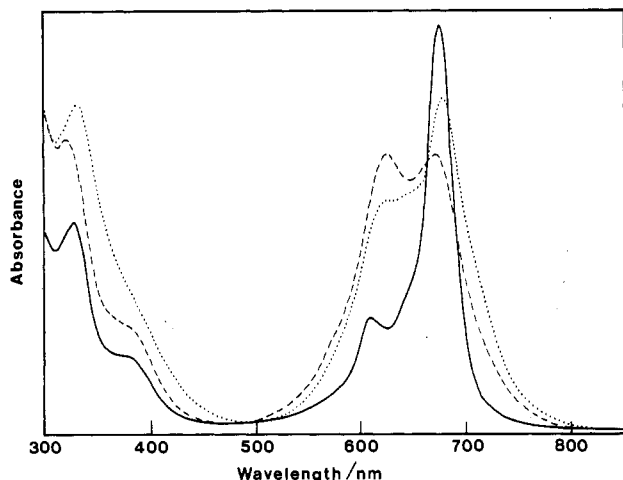


**Figure 4.** Electronic absorption spectra of  $\text{Co}^{\text{II}}\text{TNPC}(-2)$  (—),  $\text{EtMeO}(5)[\text{Co}^{\text{II}}\text{TrNPc}(-2)]_2$  (---), and  $\text{C}(2)[\text{Co}^{\text{II}}\text{TrNPc}(-2)]_2$  (···) in DCB ( $[\text{Pc}] \times \text{path length} = \text{constant}$ ).

DCB. Values of half-wave potentials measured for the binuclear complexes in DCB are given in Table I. Note that the potential of the second oxidation couple (II) is very sensitive to traces of anions that can coordinate to the cobalt atom.

No splitting of the redox peaks was seen for any of the binuclear complexes, such as has been observed for the  $\text{Co}(\text{II})/\text{Co}(\text{I})$  couple of a "clamshell" cobalt porphyrin<sup>13</sup> and the  $\text{Co}(\text{II})/\text{Co}(\text{I})$  and  $\text{Co}(\text{III})/\text{Co}(\text{II})$  couples of "face-to-face" cobalt porphyrins.<sup>13,14</sup> This splitting is attributed to interactions between the two cobalt atoms, which are held in close proximity by the ligand geometry, resulting in overlap of their  $d_{z^2}$  orbitals along the cobalt-cobalt axis. The size of the splitting is proportional to the magnitude of the interaction between the cobalt atoms. In the case of the binuclear phthalocyanines studied here, however, the two  $\text{CoTrNPc}$  units of each molecule oxidize or reduce "simultaneously", even for those species known to exist in a closed "clamshell" conformation in solution. Either electronic coupling between the cobalt atoms is not sufficient to cause an observable splitting of the couples, or more likely, in a preliminary chemical step, the more coupled conformations rearrange to a less coupled conformation, prior to the electron transfer. The electronic coupling is sufficient to be observed as a perturbation of the electronic spectra of these cobalt species.<sup>34</sup>

Note that for the "clamshell" porphyrin,<sup>13</sup> linkage occurs via bridges between two benzene rings of each porphyrin ring, thus giving a more rigid geometry than for the binuclear phthalocyanines reported here. The broadening of the redox waves of the binuclear compounds relative to  $\text{CoTNPC}$  may arise because of the mixture of isomers that is present, having slightly different redox potentials.

For comparison, half-wave potentials for the metal-free mononuclear complex,  $\text{H}_2\text{TNPC}$ , in DCB solution are also given in Table I. Two quasi-reversible one-electron reductions and two quasi-reversible one-electron oxidations are observed, corresponding to the first and second reductions and oxidations, respectively, of the phthalocyanine ring.

**Spectroelectrochemistry in DCB Solution.** Typical absorption spectra for  $\text{Co}^{\text{II}}\text{TNPC}(-2)$  and the "closed" and "open" binuclear species  $\text{EtMeO}(5)[\text{Co}^{\text{II}}\text{TrNPc}(-2)]_2$  and  $\text{C}(2)[\text{Co}^{\text{II}}\text{TrNPc}(-2)]_2$ , respectively, are shown in Figure 4. The binuclear species show an additional band centered at ca. 50 nm to the blue of the normal Q band as a result of interaction between the phthalocyanine rings through "exciton coupling".<sup>34,35</sup> Spectroscopic data for  $\text{CoTNPC}$  species are given in Table II.

Polarization of a solution of  $\text{CoTNPC}$  in DCB in the OTTLE at 200 mV negative of the first reduction couple (IV) results in the spectroscopic changes shown in Figure 5 and a change of color from blue to yellow. Isosbestic points are observed at 325, 360, 395, 557, and 692 nm. The spectrum is typical of a  $\text{Co}^{\text{I}}\text{Pc}(-2)$  species,<sup>17,19,20,39,40,43,44</sup> characterized by the appearance of a strong

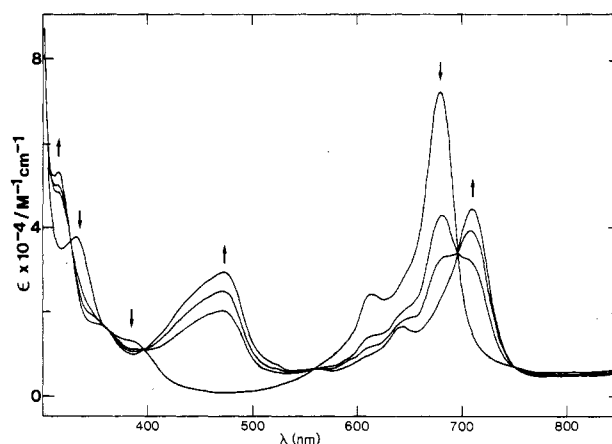


**Figure 5.** Development of the electronic absorption spectra with time during the reduction of  $\text{Co}^{\text{II}}\text{TNPC}(-2)$  at  $-1.1$  V vs  $\text{Fc}^+/\text{Fc}$  in DCB (0.3 M TBAP).  $[\text{CoTNPC}] = 1.2 \times 10^{-4}$  M.

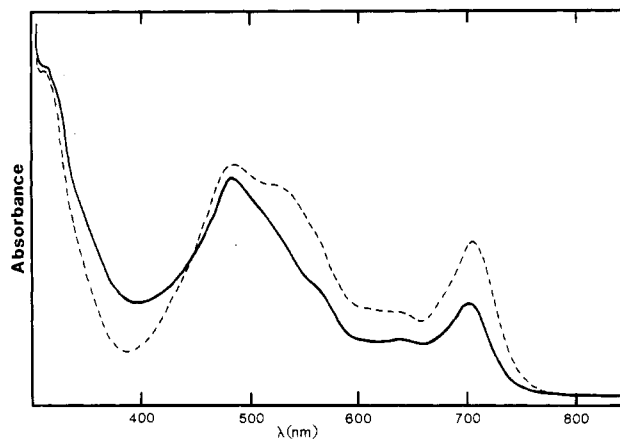


**Figure 6.** Electronic absorption spectra of electrochemically generated  $[\text{Co}^{\text{I}}\text{TNPC}(-3)]_2^{2-}$  (—) and  $\text{O}(1)[\text{Co}^{\text{I}}\text{TrNPc}(-3)]_2^{4-}$  (---) in DCB (0.3 M TBAP).  $[\text{CoTNPC}] = 9 \times 10^{-5}$  M, and  $[\text{O}(1)[\text{CoTrNPc}]_2] = 4 \times 10^{-5}$  M.

band at 475 nm, assigned as a metal-to-ligand charge transfer from  $\text{Co}^{\text{I}}\text{Pc}(-2) [d(xz, yz)] \rightarrow \pi^*(1b_{1u}) \text{Pc}(-2)$ ,<sup>40,45,46</sup> and a red shift and decrease in intensity of the Q band. The reduced species is fully reversible to the starting material by oxidation positive of the first reduction couple.

Polarization at 200 mV negative of the second reduction couple (V) results in a change from yellow to a pink solution, the spectrum of which is shown in Figure 6. The observed small red shift of the MLCT band and decrease in intensity of the Q band relative to that of the first oxidation product are similar to those obtained by Clack and Yandle<sup>20</sup> for the chemical formation of the species  $[\text{Co}^{\text{I}}\text{Pc}(-3)]_2^{2-}$  in DMF and by Le Moigne and Even<sup>43</sup> for a chemically reduced thin film of  $\text{CoPc}$ . In addition, a weak near-IR band occurs at 955 nm. The appearance of a band in the region of 950 nm appears characteristic of the ligand-reduced species, as has been observed previously for a number of metallo-phthalocyanines.<sup>20,46</sup> Reoxidation at a potential positive of couple (IV) generates the starting material with ca. 20% decrease in the Q band intensity (no decomposition products absorbing in the region of 300–1600 nm were observed).

Oxidation of  $\text{CoTNPC}$  in DCB in the OTTLE at 200 mV positive of the first oxidation couple (III), results in a rapid decrease in the intensity of the Q band and the formation of a pale pink solution. The broad, low-intensity spectrum, shown in

(43) Le Moigne, J.; Even, R. *J. Chem. Phys.* **1985**, *82*, 6472.

(44) Taube, R. *Z. Chem.* **1966**, *6*, 8.

(45) Lever, A. B. P.; Licoccia, S.; Magnell, K.; Minor, P. C.; Ramaswamy, B. S. *ACS Symp. Ser.* **1982**, *No. 201*, 237.

(46) Minor, P. C.; Gouterman, M.; Lever, A. B. P. *Inorg. Chem.* **1985**, *24*, 1894.

Table II. Electronic Absorption Maxima of CoTNPC Species

species <sup>a</sup>	$\lambda_{\max}$ nm ( $10^{-4}\epsilon$ , M <sup>-1</sup> cm <sup>-1</sup> )
[Co <sup>II</sup> TNPc(-3)] <sup>2-</sup>	315 sh
[Co <sup>II</sup> TNPc(-2)] <sup>-</sup>	313 (5.79) 330 (4.07)
[Co <sup>II</sup> TNPc(-1)] <sup>+</sup>	320 sh 320 sh 330 sh 330 sh
[Co <sup>III</sup> TNPc(0)] <sup>3+</sup>	326 (8.51)
[Co <sup>III</sup> TNPc(-2)] <sup>2+</sup>	340 sh
[Co <sup>III</sup> TNPc(-1)] <sup>2+</sup>	355 (6.31) 370 m
[Co <sup>III</sup> (CN) <sub>2</sub> TNPc(-2)] <sup>-c</sup>	355 sh
	345 sh
	350 sh
	380 (1.38)
	360 sh
	380 (2.36)
	430 br, sh
	380 sh
	355 (6.31)
	405 s
	370 m
	440 sh
	405 sh
	400 (2.40)
	495 (1.40)
	520 (1.66)
	520 sh
	520 sh
	560 vw
	560 sh
	600 sh
	620 (1.64) br
	580 sh
	620 br
	606 (3.89)
	610 (3.72)
	680 s
	610 w
	645 sh
	678 s
	640 (1.13)
	643 (1.84)
	612 (2.57)
	703 (2.35)
	708 (4.50)
	678 (7.24)
	686 (1.76)
	742 (1.15)
	668 (10.96)
	676 (14.79)
	795 m
	955 (0.32)

<sup>a</sup> In DCB solution with 0.3 M TBAP except as otherwise noted. [CoTNPC] =  $2 \times 10^{-4}$  M. Note that at these concentrations of phthalocyanine and electrolyte substantial aggregation of the Co<sup>II</sup>TNPc(-2) species occurs. Values of  $\lambda_{\max}$  ( $10^{-4}\epsilon$ ) for  $<10^{-5}$  M Co<sup>II</sup>TNPc(-2) in pure DCB are 330 (6.54), 382 (2.49), 612 (3.45), 645 sh, and 678 (13.5) nm. <sup>b</sup> DMF solution with 0.3 M TBAP. <sup>c</sup> CH<sub>3</sub>CN solution. <sup>d</sup> Key: br = broad, sh = shoulder, vw = very weak, m = medium, s = strong.

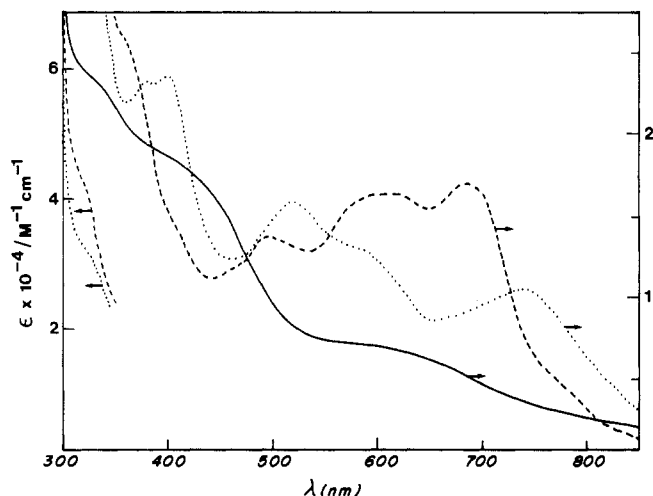


Figure 7. Electronic spectra of electrochemically generated [Co<sup>II</sup>TNPc(-1)]<sup>+</sup> (---), [Co<sup>III</sup>TNPc(-1)]<sup>2+</sup> (···), and [Co<sup>III</sup>TNPc(0)]<sup>3+</sup> (—) species in DCB (0.3 M TBAP). [CoTNPC] =  $5 \times 10^{-4}$  M.

Figure 7, is unlike those observed for cobalt(III) phthalocyanine species<sup>34,39,40,47,48</sup> but is very similar in appearance to those reported for the ligand oxidations of phthalocyanines<sup>21,22,49</sup> to form the Pc cation radical species, [Pc(-1)]<sup>+</sup>. Since this redox couple is a one-electron process, it must correspond to the one-electron oxidation of the phthalocyanine ring, to give the species [Co<sup>II</sup>TNPc(-1)]<sup>+</sup>. Similarly, a broadening and lowering of intensity of the bands in the visible region is typically observed for the ligand oxidation in metalloporphyrins.<sup>2,50-52</sup> The results are in agreement with those of Gavrillov et al.<sup>24</sup>, who reported the oxidation of Co tetra-4-*tert*-butylphthalocyanine in DCB. In contrast, the first oxidation of cobalt tetraphenylporphyrin (CoTPP) in noncoordinating solvents has been shown to occur on the cobalt atom.<sup>3-5</sup>

Polarization of the OTTLE at 200 mV positive of the second oxidation couple (II) results in the formation of a red-brown solution, with a spectrum shown in Figure 7. The broad, three-banded spectrum is typical of those found previously for chemically oxidized CoPc in CHCl<sub>3</sub><sup>47</sup> and as a thin film<sup>37</sup> and is assigned to a [Co<sup>III</sup>Pc(-1)]<sup>2+</sup> species. Thus, the second oxidation occurs on the metal to give [Co<sup>III</sup>TNPc(-1)]<sup>2+</sup>.

Polarization of the OTTLE positive of the third oxidation couple (I) gives a decrease in absorption intensity to a broad spectrum with bands centered at 430 and 630 nm, as shown in Figure 7. Rereduction of this solution negative of couple III formed the starting species with ca. 50% loss of the Q-band intensity; however, the spectrum was identical with the initial spectrum in shape, and no decomposition products absorbing in the 300-1600 nm region were observed. To our knowledge, no report has previously been made of a phthalocyanine third oxidation product. In view of the similarity of the potential to that of the second ligand oxidation of H<sub>2</sub>TNPc, and the fact that the electronic spectrum (Figure 7) is very different from the Pc(-1) species, it is likely that this is also the second ligand oxidation, to give [Co<sup>III</sup>TNPc(0)]<sup>3+</sup> rather than [Co<sup>IV</sup>TNPc(-1)]<sup>3+</sup>.

**Electrochemistry in DMF Solution.** Figure 2b shows a typical cyclic voltammogram for CoTNPC in DMF, with half-wave potentials and peak separations at 20 mV/s given in Table I. The reduction processes are very similar to those found in DCB solution, having two quasi-reversible one-electron couples separated

- (47) Homborg, H.; Kalz, W. *Z. Naturforsch., B: Anorg. Chem., Org. Chem.* **1984**, *39B*, 1490.  
 (48) Kalz, W.; Homborg, H.; Kuppers, H.; Kennedy, B. J.; Murray, K. S. *Z. Naturforsch., B: Anorg. Chem., Org. Chem.* **1984**, *39B*, 1478.  
 (49) Nyokong, T.; Gasyana, Z.; Stillman, M. J. *Inorg. Chim. Acta* **1986**, *112*, 11.  
 (50) Fuhrhop, J.-H.; Wasser, P.; Riesner, D.; Mauzerall, D. J. *Am. Chem. Soc.* **1972**, *94*, 7996.  
 (51) Dolphin, D.; Felton, R. H. *Acc. Chem. Res.* **1974**, *7*, 26.  
 (52) Fuhrhop, J.-H.; *Struct. Bonding (Berlin)* **1974**, *18*, 1.

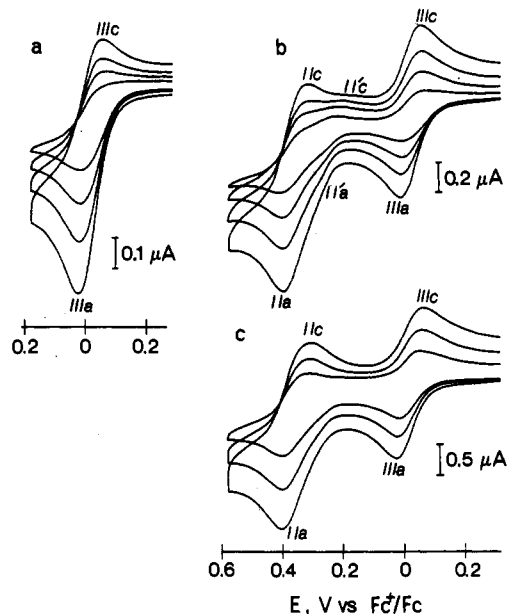


**Figure 8.** Cyclic voltammetry of CoTNPC in DMF (0.3 M TBAP) at various scan rates and switching potentials: (a) Co(III)/Co(II) couple at 2, 5, 10, and 20 mV/s; (b) Pc(-1)/Pc(-2) and Co(III)/Co(II) couples at 2, 5, 10, and 20 mV/s; (c) Pc(-1)/Pc(-2) and Co(III)/Co(II) couples at 20, 50, and 100 mV/s.  $[CoTNPC] = 1 \times 10^{-4}$  M.

by ca. 1.15 V; however, marked changes are seen for the oxidation processes. The reversibility of the first oxidation wave (III) is strongly dependent both upon scan rate and the upper positive limit of the voltage sweep. If the voltage sweep is reversed at a potential negative of the second oxidation couple (II), a broad flat irreversible return wave is obtained at slow sweep rates, which increases in magnitude with increasing sweep rate, as shown in Figure 8a.

Sweeping the potential positive of the second oxidation potential results in an increase in the return wave for a given sweep rate, although at very slow scan rates (2 mV/s) the return wave is still irreversible (Figure 8b). The second oxidation exhibits two anodic and two cathodic waves, as shown in Figure 8b. At high sweep rates (Figure 8c) (100 mV/s), the more positive wave is dominant, with only a shoulder occurring at ca. +0.3 V and a single return wave. As the sweep rate is decreased, the contribution from the more negative couple increases, so that the return wave splits into two peaks. Before the significance of these data is discussed, it is useful to review the spectroelectrochemical data.

**Spectroelectrochemistry in DMF.** Controlled-potential electrolysis in the OTTLE of a solution of CoTNPC in DMF at 200 mV positive of the first oxidation couple (III) results in the spectroscopic changes shown in Figure 9 and the formation of a blue-green solution. This spectrum, characterized by a red shift, increase in intensity and sharpening of the Q band, and a red shift of the Soret band relative to the starting spectrum, is similar to those observed for the Co<sup>III</sup>Pc species,  $[Co^{III}(X)_2Pc(-2)]^-$  (X = OH, F, Cl, or Br),<sup>47</sup>  $[Co^{III}(OH)_2TNPC(-2)]^-$ ,<sup>34</sup>  $[Co^{III}(CN)_2Pc(-2)]^-$ ,<sup>39,40,48</sup> and  $[Co^{III}(CN)_2TNPC(-2)]^-$  (this work). Thus, in DMF solution, the first oxidation (III) indeed occurs on the cobalt rather than on the phthalocyanine ring.

Polarization in the OTTLE at potentials positive of oxidation couple II resulted in a fairly rapid loss of the phthalocyanine absorption. However, the spectrum of the oxidized species was obtained by using the bulk cell/Guided Wave spectrometer arrangement. The spectrum was very similar to that of the second oxidation in DCB (see Table II), albeit with the bands red shifted by 50–90 nm with respect to those of the DCB solution. Thus couples III and II in DMF correspond to the formation of  $[Co^{III}TNPC(-2)]^+$  and  $[Co^{III}TNPC(-1)]^{2+}$ , respectively.

The binuclear cobalt phthalocyanines gave spectroelectrochemistry essentially similar to that of CoTNPC. The spectra of the redox products were those expected for complete oxidation

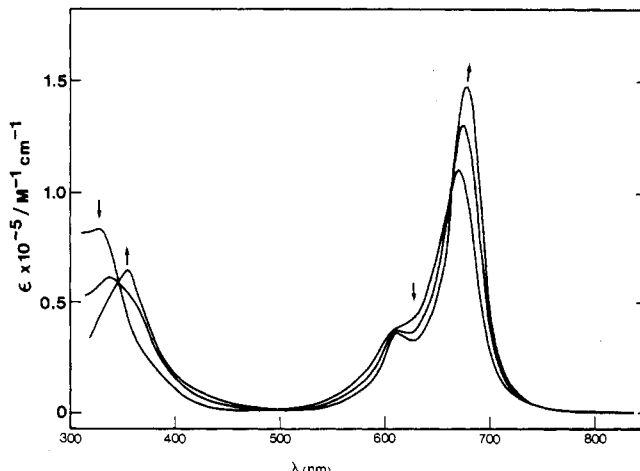


**Figure 9.** Development of the electronic absorption spectra with time during the oxidation of Co<sup>II</sup>TNPC(-2) at +0.2 V vs. Fc<sup>+</sup>/Fc in DMF (0.3 M TBAP).  $[CoTNPC] = 2.3 \times 10^{-4}$  M.

**Table III.** Cathodic to Anodic Peak Ratios for CoTNPC Redox Couple III in DMF Solution at Various Scan Rates<sup>a</sup>

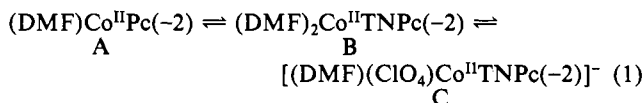
scan rate, mV/s	[TBAP], M	$i_c/i_a$	[TBAP], M	$i_c/i_a$
10			0.3	0.78
20	0.1	0.76	0.3	0.81
50	0.1	0.77	0.3	0.83
100	0.1	0.82	0.3	0.86
200	0.1	0.87		
500	0.1	1.00		

<sup>a</sup>  $[CoTNPC] = 1 \times 10^{-4}$  M. The positive switching potential lies between couples II and III.

or reduction of the two CoTrNPc units at each redox couple, with no evidence for the formation of any mixed-valence states. As an example, the spectrum of the second reduction product of O(1)[CoTrNPc]<sub>2</sub> is shown also in Figure 6. Of note, the absorption of the ligand-reduced species was rather more broad in the binuclear complexes, probably as a consequence of coupling.<sup>34</sup>

**Discussion of Electrochemical Behavior in DMF.** The bulk solute in DMF is expected to be the five-coordinate (DMF)-Co<sup>II</sup>TNPC(-2) based upon earlier studies, which show the prevalence of five-coordinate Co<sup>II</sup>Pc species.<sup>53</sup>

Since the axial site is expected to be labile, there will be other species in equilibrium. The most important are likely to be



One may readily predict that species C will oxidize at the least positive potential.<sup>18</sup> Thus in Figure 8 the anodic wave IIIa corresponds to oxidation of species C, formed very rapidly at the electrode in a CE reaction. Given that the ClO<sub>4</sub><sup>-</sup>:Co<sup>II</sup>TNPC ratio is so large and that there is an axial site vacant on the phthalocyanine, the rate of perchlorate ion incorporation is probably diffusion-controlled.

When the switching potential lies between couples II and III, the cathodic wave corresponding to wave IIIa diminishes in current quite dramatically with slower scan rate and the ratio  $i_c/i_a$  is considerably less than unity (Table III). At higher scan rates, this ratio equals unity. Thus the couple is irreversible at very slow scan rates. These ratios are subject to some uncertainty, given the close proximity of the next redox couple, so that calculation of rate constants therefrom would be unreliable. We note that, at a given scan rate, the  $i_c/i_a$  ratio increases with increasing perchlorate ion concentration, supporting the view that species

(53) Cariati, F.; Galizzioli, D.; Morazzoni, F.; Busetto, C. *J. Chem. Soc., Dalton Trans.* **1975**, 556. Cariati, F.; Morazzoni, F.; Busetto, C. *J. Chem. Soc., Dalton Trans.* **1976**, 496.

C is involved as proposed. The product on the electrode after oxidation is the six-coordinate  $[(\text{DMF})(\text{ClO}_4)\text{Co}^{\text{III}}\text{TNPC}(-2)]$ . This will participate in equilibrium 2, in which either the DMF  $[(\text{DMF})(\text{ClO}_4)\text{Co}^{\text{III}}\text{Pc}(-2)] \rightleftharpoons \text{DMF} + [(\text{ClO}_4)\text{Co}^{\text{III}}\text{Pc}(-2)]$   $\rightleftharpoons \text{ClO}_4^- + [(\text{DMF})\text{Co}^{\text{III}}\text{Pc}(-2)]^+$  (2)

or perchlorato group is lost to form a five-coordinate species that is much more readily reducible to Co(II) than is the six-coordinate species and thus has a redox potential positive of couple III. Although this five-coordinate Co(III) species is likely to be formed in only minute amounts, the equilibrium should be sufficiently facile that, during the time of the cathodic sweep positive of couple III, some of the Co(III) species on the electrode would be reduced and therefore not contribute current to cathodic wave IIIc. Clearly the slower the sweep, the greater the loss in cathodic current in wave IIIc. Previous studies<sup>54</sup> show that although axial substitution of six-coordinate Co(III) species is usually very slow indeed, axial sites on Co(III) macrocycles are more labile.

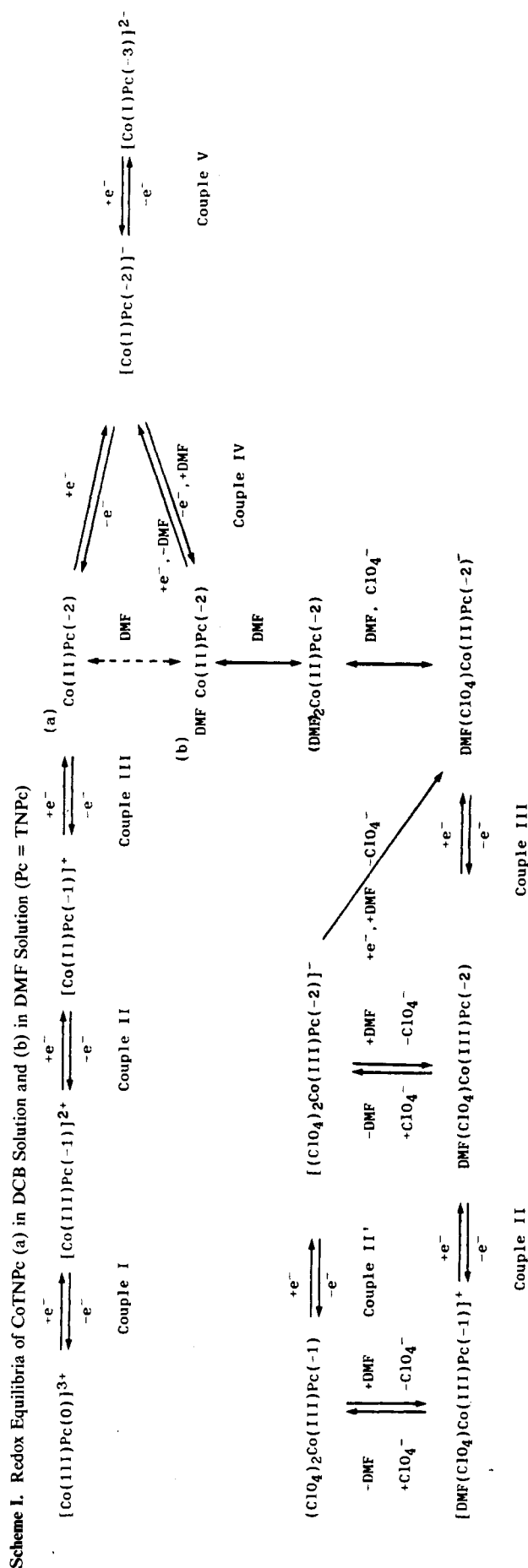
Beyond wave IIIa, the next process is oxidation to  $[(\text{DMF})(\text{ClO}_4)\text{Co}^{\text{III}}\text{TNPC}(-1)]^+$  reasonably associated with the major oxidation peak IIa. Although in the spectroelectrochemical experiment this species is unstable, it is evidently sufficiently stable in the much shorter time frame of the cyclic voltammetry experiment. There are two clearly identifiable cathodic peaks whose relative intensity changes with scan rate (Figure 8b). With increasing scan rate the more positive wave (IIc) grows at the expense of the less positive wave (II'c), and vice versa at slower scan rates. Moreover with increasing perchlorate ion concentration (0.1–0.3 M), the less positive wave grows slightly, at the expense of the more positive wave. The most positive reduction wave, wave IIc, must correspond with the reduction of  $[(\text{DMF})(\text{ClO}_4)\text{Co}^{\text{III}}\text{TNPC}(-1)]^+$ . Wave II'c must involve additional perchlorate ion and is reasonably associated with reduction of  $[(\text{ClO}_4)_2\text{Co}^{\text{III}}\text{TNPC}(-1)]$  formed by a slow substitution of DMF by perchlorate ion in  $[(\text{DMF})(\text{ClO}_4)\text{Co}^{\text{III}}\text{TNPC}(-1)]^+$ .

On the anodic component of couple II, there is a very weak lower potential shoulder, which is more evident at slow scan rates (Figure 8b) and is marginally enhanced by increasing perchlorate ion concentration. This is likely to be the anodic partner to peak II'c formed by very slow substitution of DMF by perchlorate ion in  $[(\text{DMF})(\text{ClO}_4)\text{Co}^{\text{III}}\text{TNPC}(-2)]$  formed on the electrode surface. The redox couple for the bis(perchlorato) species (couple II') lies at a (slightly) lower potential than for the mono(perchlorato) species, as would be anticipated because of the extra charge disposed onto the cobalt ion.<sup>18</sup>

When the switching potential is positive of couple II, the cathodic return wave for couple III is not diminished except at exceptionally slow scan rates, the  $i_c/i_a$  ratio remaining unity. Assuming that the above mechanism for irreversibility is correct, it follows that the species now on the electrode must be different from the previous switching situation and must dissociate a ligand rather more slowly. Indeed, at the slow scan rates necessary to observe this phenomenon, the species on the electrode when switched beyond couple II will be  $[(\text{ClO}_4)_2\text{Co}^{\text{III}}\text{TNPC}(-2)]^-$ , which must then have a slower dissociation rate. This bis(perchlorato) species would be expected to have a somewhat less positive reduction potential than the  $[(\text{DMF})(\text{ClO}_4)\text{Co}^{\text{III}}\text{TNPC}(-2)]$  species, yet this appears experimentally not to be the case. Possibly the difference is too small to be evident.

Previously, Kelly and Kadish<sup>12</sup> had shown that  $(\text{DMF})(\text{Cl})\text{Cr}^{\text{III}}\text{TTP}$  and  $[(\text{DMF})_2\text{Cr}^{\text{III}}\text{TTP}]^+$  both reduce at the same potential, in DMF, and explain this by assuming that a CE reaction occurs, with chloride being replaced by DMF at the electrode in a reaction driven by the applied potential. This is the same argument being used here to infer which cobalt species is active at each couple.

Thus, in summary, the species involved in the region of couples II and III are (vs.  $\text{Fc}^+/\text{Fc}$ ) as follows:  $[(\text{DMF})(\text{ClO}_4)\text{Co}^{\text{III}}\text{TNPC}(-1)]^+$



(54) Fleischer, E. B.; Jacobs, S.; Mestichelli, L. *J. Am. Chem. Soc.* **1968**, *90*, 2527.

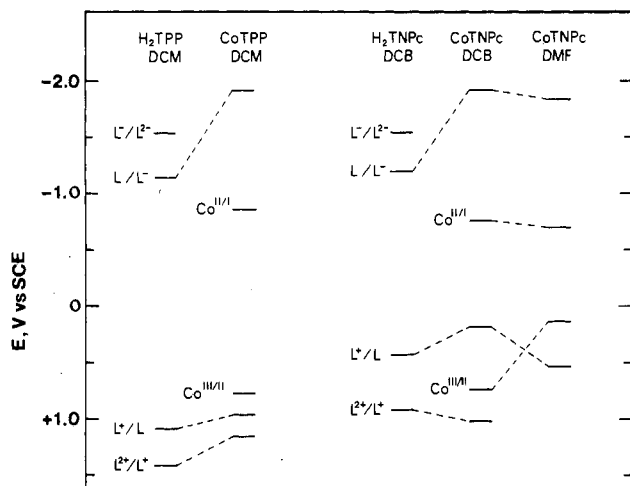


Figure 10. Summary of the electrochemistry of  $H_2TNPc$  and  $CoTNPc$  and comparison with that of  $H_2TPP$  and  $CoTPP$ .

$Co^{III}TNPc(-2)/(DMF)(ClO_4)Co^{II}TNPc(-2)^-$ ,  $E_{1/2} = -0.02$  V;  $[(DMF)(ClO_4)Co^{III}TNPc(-1)^+/(DMF)(ClO_4)Co^{II}TNPc(-2)]$ ,  $E_{1/2} = +0.38$  V;  $[(ClO_4)_2Co^{III}TNPc(-1)/(ClO_4)_2Co^{II}TNPc(-2)^-]$ ,  $E_{1/2} = +0.30$  V. The overall redox behavior is shown in Scheme I.

**Rationalization with the Literature.** There are scattered reports of the spectra of phthalocyanine anion and cation radical species in the literature, as referenced above, but this is the first study where the spectra of one species have been followed through seven oxidation states. Cation radical spectra have only rarely been reported in the solution state.

It is tempting to try to assign the spectra of the various oxidation species reported here and compare the data with those for related materials in the literature. Indeed we have previously predicted the type of spectra to be anticipated for metallophthalocyanines in various oxidation states;<sup>46</sup> however, in the absence of supporting data such as MCD,<sup>49</sup> it would be foolhardy to try to assign, in any detail, the rather broad and overlapping bands commonly observed for these various species (e.g. Figure 7).

Phthalocyanine cation radical  $Pc(-1)$  spectra are now known for a range of central substituents including  $Co(II)$ ,  $Co(III)$ ,  $Ru(II)$ ,  $Rh(III)$ ,  $Fe(III)$ ,  $Cr(III)$ ,  $Zn(II)$ ,  $Si(IV)$ ,  $H_2$ ,  $Mg(II)$ , and  $Cu(II)$ .<sup>21,22,37,46,47,49,55,56</sup> These all appear to show medium-intensity bands near 700–800 nm and near 500 nm. The former is assigned as a transition from a lower lying  $e_g$   $\pi$  level into the hole in the HOMO  $\pi$  level.<sup>46,49,55</sup> Charge-transfer spectra from metal d levels to the hole in the HOMO level can be anticipated but have not been identified.<sup>49</sup>

The voltammetry of  $H_2TNPc$  and  $CoTNPc$  is summarized and compared with that of  $H_2TPP$ <sup>8,9,11,15,16,57–59</sup> and  $CoTPP$ <sup>3–8,15,16,58</sup> in the form of a redox potential state diagram in Figure 10.

Complexation with cobalt(II) causes a negative shift in the potential of the first ligand reduction by ca. 500 mV in noncoordinating solvents for both  $TNPc$  and  $TPP$  (Figure 10), as a result of the insertion of the cobalt d orbitals between the HOMO and LUMO orbitals of the ring. The potential of the first ligand oxidation also shifts negatively, but to a lesser extent, resulting in a net increase in separation between the first oxidation and reduction couples ( $E(L^+/L) - E(L/L^-) = 2.1$  and 2.9 V for  $CoTNPc$  and  $CoTPP$ , respectively).<sup>3–5,7,8,58</sup> Notably, the  $L/L^-$ ,  $Co(II)/Co(I)$ , and  $Co(III)/(II)$  couples of  $CoTNPc$  and  $CoTPP$  lie at similar potentials in noncoordinating solvents (Figure 10). For both compounds, the  $Co(II)/Co(I)$  couple lies positive of the first ligand reduction, so that the cobalt is reduced first. However, differences are seen in the oxidation processes. For  $CoTNPc$ , the separation between the HOMO and LUMO orbitals of the ring is small enough to leave the  $L^+/L$  couple negative of the  $Co(III)/Co(II)$  couple, so that oxidation occurs at the ring first. For  $CoTPP$ , however, the larger separation of the HOMO and LUMO orbitals results in the  $L^+/L$  couple lying positive of the  $Co(III)/Co(II)$  couple, even in noncoordinating solvents. The relative positions of the cobalt d orbitals and  $TNPc$  HOMO also results in a large increase in separation of the first and second ligand oxidations compared with the metal-free complex, while for porphyrins a small decrease in separation of the couples is seen.<sup>4,5,7,11,15,16</sup>

In DMF, the  $Co(III)/Co(II)$  couple of  $CoTNPc$  shifts negatively by ca. 600 mV, as a result of the stabilization of the  $Co(III)$  species in the presence of the axially coordinating solvent, while the  $L^+/L$  couple shifts positively by 300 mV, as a consequence of the presence of the highly polarizing central ion ( $Co(III)$ ).<sup>60</sup> Thus, the first oxidation now occurs at the cobalt atom. Similarly, the  $Co(III)/Co(II)$  couple shifts negatively by almost 800 mV for  $CoTPP$  on going from DCM to DMF solution.<sup>4</sup> The potential of the  $Co(II)/Co(I)$  couple remains approximately constant, as expected for the four-coordinate  $Co(I)$  species.

Data for the binuclear species are somewhat disappointing given that they differ little from the mononuclear analogue. The binuclear species are significantly, but not dramatically, more efficient for oxygen reduction<sup>26</sup> than the mononuclear control. More tightly coupled binuclear phthalocyanines are currently under investigation.

**Acknowledgment.** The authors are indebted to the Natural Sciences and Engineering Research Council (Ottawa, Canada) and the Office of Naval Research (Washington, DC) for financial support.

**Registry No.**  $[Co^I TNPc(-3)]^{2-}$ , 106138-94-7;  $[Co^I TNPc(-2)]^-$ , 106138-95-8;  $[Co^{II} TNPc(-2)]$ , 93581-77-2;  $[Co^{II} TNPc(-1)]^+$ , 106138-96-9;  $[Co^{III} TNPc(-1)]^{2+}$ , 106138-97-0;  $[Co^{III} TNPc(0)]^{3+}$ , 106138-98-1;  $H_2 TNPc^{2-}$ , 106095-22-1;  $H_2 TNPc^-$ , 106095-23-2;  $H_2 TNPc$ , 93673-00-8;  $H_2 TNPc^+$ , 106188-53-8;  $H_2 TNPc^{2+}$ , 106095-25-4;  $EtMeO(5)-[CoTrNPc]_2$ , 97251-73-5;  $Cat(4)[CoTrNPc]_2$ , 99293-00-2;  $C(2)-[CoTrNPc]_2$ , 99279-29-5;  $O(1)[CoTrNPc]_2$ , 106138-92-5;  $[Co^{III}(CN)_2 TNPc]^-$ , 106138-99-2;  $(DMF)(ClO_4)Co^{III} TNPc(-2)$ , 106139-00-8;  $(DMF)(ClO_4)Co^{III} TNPc(-2)^-$ , 106160-83-2;  $(DMF)(ClO_4)Co^{III} TNPc(-1)^+$ , 106139-01-9;  $(ClO_4)_2Co^{III} TNPc(-1)$ , 106139-02-0;  $(ClO_4)_2Co^{III} TNPc(-2)^-$ , 106139-03-1;  $O(1)[Co^I TrNPc(-3)]_2^{4-}$ , 106138-93-6.

(55) Nyokong, T.; Gasyna, Z.; Stillman, M. J., private communication.

(56) Homborg, H. Z. *Anorg. Allg. Chem.* **1983**, *507*, 35.

(57) Kadish, K. M.; Thompson, L. K.; Beroiz, D.; Bottomley, L. A. *ACS Symp. Ser.* **1977**, *38*, 51.

(58) Wolberg, A. *Isr. J. Chem.* **1974**, *12*, 1031.

(59) Lexa, D.; Reix, M. *J. Chim. Phys.* **1974**, *71*, 511.

(60) Lever, A. B. P.; Minor, P. C. *Inorg. Chem.* **1981**, *20*, 4015.